

# Could $M_{T2}$ be a singularity variable?

Chan Beom Park\*

*Center for Theoretical Physics of the Universe, Institute for Basic Science (IBS),  
55 Expo-ro, Yuseong-gu, Daejeon 34126, Korea*

## Abstract

The algebraic singularity method is a framework for analyzing collider events with missing energy. It provides a way to draw out a set of singularity variables that can catch singular features originating from the projection of full phase space onto the observable phase space of measured particle momenta. It is a promising approach applicable to various physics processes with missing energy but still requires more studies for use in practice. Meanwhile, in the double-sided decay topology with an invisible particle on each side, the  $M_{T2}$  variable has been known to be a useful collider observable for measuring particle masses from missing energy events or setting signal regions of collider searches. We investigate the relation between the two different types of kinematic variables in double-sided decay topology. We find that the singularity variables contain the  $M_{T2}$  variable in many cases, although the former is not a strict superset of the latter.

arXiv:2108.13820v2 [hep-ph] 9 Nov 2021

---

\*E-mail: [cbpark@ibs.re.kr](mailto:cbpark@ibs.re.kr)

---

# Contents

<b>1</b>	<b>Introduction</b>	<b>1</b>
<b>2</b>	<b>The <math>M_{T2}</math> variable</b>	<b>3</b>
<b>3</b>	<b>Algebraic singularity method</b>	<b>7</b>
3.1	Singularity variable for double-sided decay topology . . . . .	10
<b>4</b>	<b>Comparison of <math>M_{T2}</math> and singularity variables</b>	<b>13</b>
4.1	Beyond trivial zero . . . . .	19
<b>5</b>	<b>Conclusions</b>	<b>20</b>
	<b>References</b>	<b>21</b>

---

## 1 Introduction

The  $M_{T2}$  variable was devised to measure supersymmetric particle masses in collider events with missing energy due to invisible particles in the final state [1, 2]. Although the discovery of supersymmetry remains to be made, the  $M_{T2}$  variable has served as the main observable in various physics analyses at hadron colliders from the measurement of top quark mass and properties [3–6] to the searches for supersymmetric particles [7–9]. It has also directly influenced the inventions of other kinematic methods and variables such as the  $M_{T2}$ -assisted on-shell (MAOS) method [10],  $M_{CT2}$  [11], and  $M_2$  [12]. We will present a brief review of the  $M_{T2}$  variable in Sec. 2.

Considering that the invention of the  $M_{T2}$  variable started from the attempt of generalizing the transverse mass [13, 14] to deal with two identical decay chains, the algebraic singularity method has emerged from the realization that the phase space of particle momenta is the solution space of the system of kinematic constraints [15]. At collider experiments, we detect only visible particle momenta while missing invisible ones. It can be regarded as the projection of the full phase space of collider event onto the visible subspace. The algebraic singularity method proposes that one can construct singularity variables, which unveil singularities caused by the projection of phase space, by exploiting all the available kinematic constraints in a specific way. Compared to the  $M_{T2}$  variable, the algebraic singularity method is a general framework applicable to any decay topology of physics processes containing invisible particles in the final state. The formal description of the algebraic singularity method and the singularity variables are given in Sec. 3.

The author of Ref. [15] mentioned that the algebraic singularity method was initiated due to his desire to understand the  $M_{T2}$  variable, and he could eventually derive the  $M_{T2}$  variable by using the algebraic singularity method [16]. However, in Ref. [15], the

relation between the  $M_{T2}$  variable and the algebraic singularity method was not elucidated, and it has never been considered in the following works by different authors [17–20]. Moreover, in Ref. [21], it has even been argued that  $M_{T2}$  is not associated with the singularity variables. On the other hand, in other studies, it has been realized that  $M_{T2}$  is not an ad hoc variable, but it sets a boundary of the mass region consistent with the kinematic constraints, which are indeed the defining polynomials of phase space that are used in the algebraic singularity method [22, 23]. These seemingly discrepant arguments and claims have motivated us to examine the relation between the  $M_{T2}$  variable and the corresponding singularity variables. If they turn out to be truly orthogonal, the algebraic singularity method will provide new kinematic variables that can be employed in the physics analyses where either or both of the  $M_{T2}$  variable and the new variables are applicable. Otherwise, if they are related to each other in any manner, it may still lead to a deeper understanding of the methods. Either way, the algebraic singularity method is an interesting framework for studying various decay topologies with missing energy. We investigate the relation between the  $M_{T2}$  and the singularity variable in Sec. 4. Then, the final section is devoted to conclusions.

Before embarking on a discussion of the above issues, a few comments are in order on the applicability of the algebraic singularity method to physics analyses at colliders. As mentioned above, the algebraic singularity method is, in principle, a framework for analyzing the collider events of any decay topology with missing energy rather than a collider variable designed for specific physics processes. The method is still widely unknown and largely unexplored in physics community due to its use of abstract mathematics and the lack of concrete prescriptions with practical examples. A set of worked-out examples of deriving the singularity variables using the method has appeared only very recently [19]. One way to appreciate the potential of the method would be to compare the singularity variables with the known collider variables. In a single two-body decay with an invisible particle in the final state, it has been shown that the well-known transverse mass [13, 14] can be derived by using the method [17–19, 24]. We will show the derivation of the transverse mass in Sec. 3 by using the Gröbner basis as proposed in the original literature [15] to help the reader understand the method. It has also been found that the  $\Delta_4$  observable [25, 26], appearing as a factor in four-body phase space [27], corresponds to the singularity variable [19]. We anticipate that our attempt of comparing the  $M_{T2}$  with the singularity variables in double-sided decay topology will also help the reader to gain an understanding of the method and to apply the method to find the signals of unexplored decay topologies at colliders.

Though we will not pursue here, there is room for improvement in the way of identifying the singularities of phase space. As noted above, the algebraic singularity method is to capture the kinematic singularities caused by the projection of the full phase space onto the visible subspace. In the original literature, it has been argued that the Gröbner basis of kinematic constraint equations would be particularly useful for identifying singular points on the visible subspace. Meanwhile, the other following works [17–20] have obtained the singularity variables without employing Gröbner bases. As will be seen in Sec. 3, Gröbner bases have a useful property for identifying singularities. However, the expressions appear to be much more complex than the original system of kinematic

constraints, and computing Gröbner bases can be challenging, depending on the form and the numbers of the polynomial equations. We may attempt a different formulation of the method by systematically transforming the system of kinematic constraints into a more refined space of polynomial equations that one can more handily extract singularities. Another possible direction worth exploring is to combine the method with machine learning techniques. The singularity variables can be used as input features for training collider data, and it is conceivable to devise an architecture encoding the algorithm for finding the singularities. We stress that there is much more to explore in further developments and finding the applications of the algebraic singularity method to collider data analyses.

## 2 The $M_{T2}$ variable

We begin our discussion with the definition and the properties of the  $M_{T2}$  variable before looking into the algebraic singularity method. The  $M_{T2}$  variable was devised as a generalization of the transverse mass for measuring the masses of supersymmetric particles produced in a pair at hadron colliders, and hence it is often called the *transverse mass* in literature. Supersymmetric processes yield missing energy events if the lightest supersymmetric particle is electrically neutral and stable on a time scale well beyond the scale of the detector. The processes typically have the decay topology of

$$Y + \bar{Y} + U \longrightarrow v_1(p_1)\chi(k_1) + v_2(p_2)\bar{\chi}(k_2) + U(u), \quad (2.1)$$

where  $v_1$  and  $v_2$  are visible objects such as charged leptons and jets, and  $\chi$  is the invisible particle corresponding to the culprit responsible for the missing energy. For example, consider the process of pair-produced gluinos, each of which decays into the final state of two quarks plus the lightest neutralino,  $\tilde{g}\tilde{g} \rightarrow q\bar{q}\tilde{\chi}_1^0 + q'\bar{q}'\tilde{\chi}_1^0$ . In this process,  $v_1$  and  $v_2$  correspond to the two-quark-jet systems, and  $\chi$  is the invisible neutralino. Hereafter, the index  $a = 1, 2$  denotes each side of the decays in (2.1).  $U$  is the upstream-momentum object, which is not associated with the decays of  $Y$  and  $\bar{Y}$ , such as initial state radiation. We will take into account the effect of upstream momentum in Sec. 4. In this article, we assume that the decay topology is symmetric, i.e.,  $M_Y = M_{\bar{Y}}$  and  $M_\chi = M_{\bar{\chi}}$ .

For the double-sided decay topology (2.1) and the hypothesized invisible particle mass  $M_\chi$ , the  $M_{T2}$  variable is defined as

$$M_{T2} \equiv \min_{\mathbf{k}_{1T}, \mathbf{k}_{2T} \in \mathbb{R}^2} \left[ \max \left\{ M_{1T}(p_{1T}, k_{1T}, M_\chi), M_{2T}(p_{2T}, k_{2T}, M_\chi) \right\} \right] \\ \text{subject to } \mathbf{k}_{1T} + \mathbf{k}_{2T} = \mathbf{P}_T, \quad (2.2)$$

where  $M_{aT}$  are transverse masses given by

$$M_{aT}(p_{aT}, k_{aT}, M_\chi) = \left[ m_a^2 + M_\chi^2 + 2 \left( E_{aT} e_{aT} - \mathbf{p}_{aT} \cdot \mathbf{k}_{aT} \right) \right]^{1/2} \quad (2.3)$$

for the final-state particle momenta projected onto the  $(1+2)$ -dimensional space:

$$p_{aT} = (E_{aT}, \mathbf{p}_{aT}), \quad k_{aT} = (e_{aT}, \mathbf{k}_{aT}). \quad (2.4)$$

Here,  $E_{aT} = (m_a^2 + \|\mathbf{p}_{aT}\|^2)^{1/2}$  and  $e_{aT} = (M_\chi^2 + \|\mathbf{k}_{aT}\|^2)^{1/2}$  are transverse energies, and  $m_a^2 = p_a^2$ . As will be seen shortly,  $\mathbf{k}_{aT}$  in Eq. (2.3) are not the true invisible momenta, nor inputs inserted by hand, but are determined by the minimization of the objective function of  $M_{T2}$  under the constraint on the missing transverse momentum,

$$\mathbf{P}_T = -\mathbf{p}_{1T} - \mathbf{p}_{2T} - \mathbf{u}_T. \quad (2.5)$$

Therefore, the  $M_{T2}$  variable is a function of visible particle momenta  $p_a$ , missing transverse momentum  $\mathbf{P}_T$ , and the guessed value of invisible particle mass  $M_\chi$ . What makes the  $M_{T2}$  variable useful for mass measurement is that if one inserts a correct value of  $M_\chi$ , its distribution has an endpoint at the parent particle mass,  $M_Y$ :

$$M_{T2}(M_\chi = M_\chi^{\text{true}}) \leq M_Y. \quad (2.6)$$

Because the  $M_{T2}$  variable is constructed by only kinematic quantities, it applies to any process, not only the supersymmetric ones, as long as the decay topology given in (2.1) can describe the process of interest.

The calculation of the  $M_{T2}$  variable corresponds to the *constrained* minimization problem of the objective function,

$$f(\mathbf{k}_{aT}) = \max \left\{ M_{1T}(k_{1T}), M_{2T}(k_{2T}) \right\}, \quad (2.7)$$

subject to the equality constraint given by

$$\mathbf{c}(\mathbf{k}_a) = \mathbf{k}_{1T} + \mathbf{k}_{2T} - \mathbf{P}_T = \mathbf{0}. \quad (2.8)$$

The problem can be made simpler by eliminating  $\mathbf{k}_{2T}$  using the constraint (2.8),  $\mathbf{k}_{2T} = \mathbf{P}_T - \mathbf{k}_{1T}$ . Then, the objective function becomes

$$f(\mathbf{k}_{1T}) = \max \left\{ M_{1T}(e_{1T}, \mathbf{k}_{1T}), M_{2T}(e_{2T}, \mathbf{P}_T - \mathbf{k}_{1T}) \right\}, \quad (2.9)$$

where  $e_{2T} = (M_\chi^2 + \|\mathbf{P}_T - \mathbf{k}_{1T}\|^2)^{1/2}$ . The calculation of  $M_{T2}$  has now become an *unconstrained* minimization on a function of two variables,  $\mathbf{k}_{1T} = (k_{1x}, k_{1y})$ . The value of  $\mathbf{k}_{1T}$  at the minimum of the objective function  $f(\mathbf{k}_{1T})$  is the  $M_{T2}$  solution to the invisible particle momenta,

$$\tilde{\mathbf{k}}_{1T} = \underset{\mathbf{k}_{1T} \in \mathbb{R}^2}{\operatorname{argmin}} f(\mathbf{k}_{1T}). \quad (2.10)$$

Here, *argmin* stands for the argument of minimum, i.e., the point  $\mathbf{k}_{1T}$  for which  $f(\mathbf{k}_{1T})$  attains its minimum. It has been found that  $\tilde{\mathbf{k}}_{1T}$  can provide a good approximation to the invisible particle momenta along with on-shell mass constraints [10]. Even though we have converted to a simpler problem of unconstrained minimization over the fewer degrees of freedom, one should employ a numerical algorithm, such as the quasi-Newton method, to obtain the value of  $M_{T2}$ . We refer the reader to Refs. [28, 29] for a review of the  $M_{T2}$  variable in terms of minimization problems and the numerical algorithms feasible for solving the problem.

Although we use numerical algorithms in practical physics analyses, it is worth inspecting the analytic property of the  $M_{T2}$  variable. Because the objective function

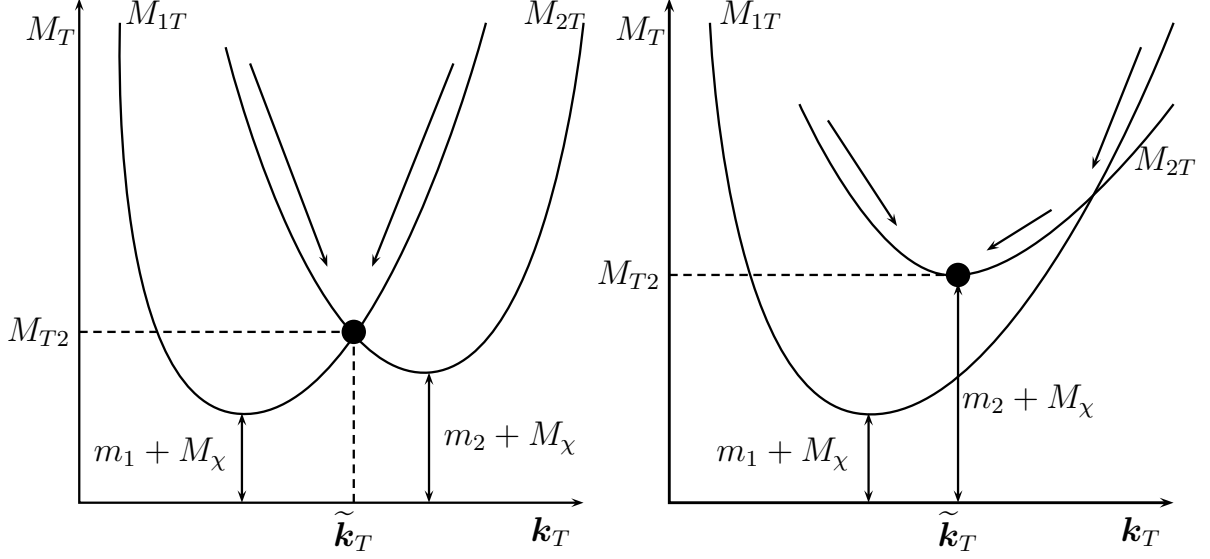


Figure 1: Schematic pictures of  $M_{T2}$  for the balanced (left) and the unbalanced (right) configurations of transverse masses. The black dot in each plot corresponds to the  $M_{T2}$  value obtained by minimization over the invisible particle momenta  $\mathbf{k}_T$ , and  $\tilde{\mathbf{k}}_T$  is the solution (or the minimizer) of  $M_{T2}$ .

of  $M_{T2}$  is a convex function over the invisible particle momenta  $\mathbf{k}_{aT}$  [29, 30], it has a unique local minimum, which is automatically a global minimum. Furthermore, as the transverse masses in Eq. (2.3) are also convex functions, the  $M_{T2}$  value is determined by the configuration of the two convex functions, as depicted in Fig. 1. The stationary points of the transverse masses can be obtained by requiring their gradients,

$$\begin{aligned} \frac{\partial M_{1T}^2}{\partial \mathbf{k}_{1T}} &= 2 \left[ \frac{E_{1T}}{e_{1T}} \mathbf{k}_{1T} - \mathbf{p}_{1T} \right], \\ \frac{\partial M_{2T}^2}{\partial \mathbf{k}_{1T}} &= 2 \left[ -\frac{E_{2T}}{e_{2T}} (\mathbf{P}_T - \mathbf{k}_{1T}) + \mathbf{p}_{2T} \right], \end{aligned} \quad (2.11)$$

to be vanishing. Here, we have eliminated  $\mathbf{k}_{2T}$  by using the constraint on missing transverse momentum given in Eq. (2.8). At each stationary point, we have the global minimum of corresponding transverse mass as follows:

$$\begin{aligned} M_{1T} &= m_1 + M_\chi \quad \text{when } \mathbf{k}_{1T} = \frac{e_{1T}}{E_{1T}} \mathbf{p}_{1T}, \\ M_{2T} &= m_2 + M_\chi \quad \text{when } \mathbf{k}_{1T} = \mathbf{P}_T - \frac{e_{2T}}{E_{2T}} \mathbf{p}_{2T}. \end{aligned} \quad (2.12)$$

The configuration of the transverse masses are determined by the visible particle momenta and missing transverse momentum. In the configuration depicted in the left panel of Fig. 1, the  $M_{T2}$  value is given by

$$M_{T2} = M_{1T} = M_{2T} \quad (2.13)$$

if both conditions below are satisfied:

$$M_{2T} \geq m_1 + M_\chi \quad \text{when } \mathbf{k}_{1T} = \frac{e_{1T}}{E_{1T}} \mathbf{p}_{1T},$$

$$M_{1T} \geq m_2 + M_\chi \quad \text{when } \mathbf{k}_{1T} = \mathbf{P}_T - \frac{e_{2T}}{E_{2T}} \mathbf{p}_{2T}. \quad (2.14)$$

This is called the *balanced* configuration. Otherwise, if any of the conditions is violated, the  $M_{T2}$  value is given by the larger of the two global minima of the transverse masses,

$$M_{T2} = \max \left[ m_1 + M_\chi, m_2 + M_\chi \right]. \quad (2.15)$$

See the right panel of Fig. 1. In this case, Eq. (2.13) does not hold, and it is termed the *unbalanced* configuration. The balanced and the unbalanced configurations span all possible cases of the  $M_{T2}$  solution: an event can be in either a balanced or an unbalanced configuration.

The general analytic expression of  $M_{T2}$  in balanced configurations is hitherto unknown except for some special cases [31–35], whereas the expression of the  $M_{T2}$  variable in the case of the unbalanced configuration is given by Eq. (2.15).<sup>1</sup> When the upstream momentum in the decay topology (2.1) is vanishing, the expression of  $M_{T2}$  in balanced configurations has been identified, and it is given as follows [31, 32]:

$$M_{T2}^2 = M_\chi^2 + A_T + \sqrt{\left(1 + \frac{4M_\chi^2}{2A_T - m_1^2 - m_2^2}\right) (A_T^2 - m_1^2 m_2^2)}, \quad (2.16)$$

where

$$A_T = E_{1T} E_{2T} + \mathbf{p}_{1T} \cdot \mathbf{p}_{2T}. \quad (2.17)$$

Likewise, the analytic expression of the  $M_{T2}$  solution,  $\tilde{\mathbf{k}}_{1T}$ , applicable in all respects, remains to be identified. In the case of vanishing upstream momentum, the derivation of the  $M_{T2}$  solution is capable but quite involved [41]. Nonetheless, in the plain case where the visible particles are massless,  $m_1 = m_2 = 0$ , we can use a simple ansatz for the form of the  $M_{T2}$  solution in the balanced configuration, given as follows:

$$\tilde{\mathbf{k}}_{1T} = \frac{1}{2} \left[ (\alpha_T - 1) \mathbf{p}_{1T} - (\alpha_T + 1) \mathbf{p}_{2T} \right], \quad (2.18)$$

where  $\alpha_T$  is a function of the visible particle momenta and the invisible particle mass  $M_\chi$ . By substituting the above expression into

$$M_{T2}^2 = \frac{M_{1T}^2 + M_{2T}^2}{2} \quad (2.19)$$

and using the expression of  $M_{T2}$  in Eq. (2.16) with  $m_1 = m_2 = 0$ , we get

$$\alpha_T = \sqrt{1 + \frac{2M_\chi^2}{A_T}}. \quad (2.20)$$

Here,  $A_T = \|\mathbf{p}_{1T}\| \|\mathbf{p}_{2T}\| + \mathbf{p}_{1T} \cdot \mathbf{p}_{2T}$ . If the invisible particle is massless as well,  $M_\chi = 0$ , the expression (2.18) further simplifies as

$$\tilde{\mathbf{k}}_{1T} = -\mathbf{p}_{2T}. \quad (2.21)$$

---

<sup>1</sup>On the other hand, the analytic expressions for the endpoint of the  $M_{T2}$  distribution are known [32, 36–40].

Because we here assume that the upstream momentum is vanishing, the missing transverse momentum is given by the negative vector sum of the visible particle momenta from the decays of  $Y$  and  $\bar{Y}$ ,  $\vec{\mathbf{P}}_T = -\mathbf{p}_{1T} - \mathbf{p}_{2T}$ . Therefore, the invisible transverse momentum of the second decay chain is given by

$$\tilde{\mathbf{k}}_{2T} = -\mathbf{p}_{1T}. \quad (2.22)$$

This expression matches that identified in the study of  $M_{T2}$  for the  $h \rightarrow WW \rightarrow \ell^+ \nu \ell^- \bar{\nu}$  process, where the visible and invisible particles in the final state are all massless [42, 43]. We will revisit the fully massless case in the last section before conclusions.

### 3 Algebraic singularity method

In this section, we describe the algebraic singularity method and then turn to the discussion of the singularity variable in the double-sided decay topology (2.1). The algebraic singularity method was initiated from the realization that the phase space of final-state particle momenta is an affine variety in mathematics [15]. Let  $g_i$  be the polynomials of kinematic constraints such as energy-momentum conservation and on-shell mass relations. The total degrees of the polynomials  $g_i$  are at most two. The final-state particle momenta  $P_j$  reside in the set of all solutions of the polynomial equations,

$$\Pi(g_1, \dots, g_m) = \{(P_1, \dots, P_n) \in \mathbb{E}^n \mid g_i(P_1, \dots, P_n) = 0 \text{ for all } 1 \leq i \leq m\}, \quad (3.1)$$

where  $\mathbb{E}$  is the four-dimensional pseudo-Euclidean space,  $\mathbb{R}^{1,3}$ .

In missing energy events, not only in the double-sided decay topology, the phase space can be decomposed into  $\{(k_a, p_b)\}$ . By measuring the visible particle momenta  $p_b$  while missing the invisible particle momenta  $k_a$ , the phase space is projected onto the visible subspace  $\{p_b\}$ . The projection leads to *singularities* in the visible subspace, where the full phase space  $\{(k_a, p_b)\}$  is folded. The event number density changes abruptly at the singularities, and they can appear in several different forms such as wall or cusp.

The salient point of the algebraic singularity method is that the singularities can be identified by constructing the Jacobian matrix of the constraint polynomials  $g_i$ ,

$$J_{ij} = \frac{\partial g_i}{\partial k_j}. \quad (3.2)$$

Here, the index  $j$  runs over the energy-momentum components of the invisible particles,  $k_a = (e_a, k_{ax}, k_{ay}, k_{az})$ . The algebraic singularity method is based on the observation that the Jacobian matrix (3.2) has *reduced rank* at singularities. In other words, one or more row vectors of the Jacobian matrix are linearly dependent at singularities. Note that the Jacobian matrix defines a linear mapping, which best approximates  $g_i$  at the point  $k_a$ . If the Jacobian matrix has reduced rank, its image of the linear mapping is smaller, and the approximation by the mapping is no more valid. Consequently, having reduced rank indicates a singular behavior of  $g_i$  near the point  $k_a$ . In the subsequent works by different authors [17–20], the reduced rank condition has been referred to as “singularity condition.” The Jacobian matrix is a square matrix if the number of polynomials in



Eq. (3.1) equals to that of unknowns. In this case, the reduced rank condition is equivalent to the vanishing determinant of the Jacobian matrix, as studied in Refs. [19, 20].

In general, the defining polynomials of phase space form a system of nonlinear coupled equations, and consequently, finding the reduced rank condition of the Jacobian matrix is a nontrivial task. Affine varieties are defined by ideals, which are the sets of all polynomials having the same solution space. The ideal generated by a finite set of polynomials is analogous to the span of a finite number of vectors in linear algebra. Indeed, the finite set of polynomials is termed a *basis* of the ideal. A given ideal may have many different bases. In Ref. [15], it is emphasized that Gröbner bases, also known as the standard bases, can be particularly useful for examining the reduced rank condition of the Jacobian matrix because it can make the matrix a row echelon form. It is analogous to Gaussian elimination for linear systems. Then, to identify the singularities, we set some of the diagonal components of the Jacobian matrix in the Gröbner basis to be vanishing and check whether the row vectors of the Jacobian matrix with vanishing diagonal component are linearly dependent. Unfortunately, the analytic calculation of Gröbner bases can be challenging if the number of polynomials is large, and thus one typically employs dedicated algorithms such as Buchberger’s algorithm [44]. In the case of the double-sided decay topology in (2.1), we can manage to obtain the corresponding Gröbner basis analytically, as done in Ref. [15]. We will see the expressions of the Gröbner basis in the following subsection.

Having identified the singularities by imposing the reduced rank condition, we can construct an optimized kinematic variable, named *singularity coordinate*. It is required to be zero at singularities and is perpendicular to the singularity hypersurface in the visible phase space. Collider events near the singularities are projected onto the coordinate. It is also normalized so that the events with the same distance to the singularities give the same value. It is called a *coordinate* as it determines the positions of collider events on the singularity hypersurface. Singularity coordinate is an implicit variable because it depends on the masses of the unknown particles such as  $Y$  and  $\chi$  in the decay topology (2.1). If trial mass values have correctly been chosen, the singularity coordinate maximizes singular features. Consequently, we can deduce the mass spectrum of unknown particles by comparing several competing hypotheses using the singularity coordinate.

Although the formal definition of singularity coordinates is given in Ref. [15], it lacks a practical recipe for constructing them. It has later been supplemented by the studies of applying the algebraic singularity method to several physics processes of various decay topologies: single  $W$  production  $W \rightarrow \ell\nu$  [17], the dileptonic Higgs channel  $h \rightarrow WW \rightarrow \ell^+\nu\ell^-\bar{\nu}$  [18], heavy Higgs boson decaying to a top-quark pair  $H/A \rightarrow t\bar{t} \rightarrow bW\bar{b}W \rightarrow b\ell^+\nu\bar{b}\ell^-\bar{\nu}$  [20], and various single- and double-sided decay topologies [19]. In the studies, singularity coordinates are called interchangeably with *singularity variables*. The latter are also functions of visible particle momenta and unknown particle masses, but it has mass dimension one. The singularity variables enable us directly to measure the unknown particle masses by identifying the peak or the endpoints of their distributions. By contrast, the singularity coordinates can have mass dimensions much higher than one, and one can estimate the unknown particle masses by performing template fitting of the distribution shapes. We can hardly extract the mass information directly from the

distribution. Therefore, singularity variables are more straightforward and intuitive to use in physics analyses than singularity coordinates. In this article, we distinguish the singularity coordinates and the singularity variables and concentrate on the latter.

Before examining the singularity variable for the double-sided decay topology in (2.1), we take a look into the singularity variable for the simpler decay topology in order to help facilitate the understanding of the algebraic singularity method. Consider a single-sided two-body decay topology, where one of the decay products is invisible,

$$Y \longrightarrow v(p)\chi(k). \quad (3.3)$$

The kinematic constraints of the decay topology are given as follows:

$$\begin{aligned} k^2 &= M_\chi^2, \\ (p+k)^2 &= M_Y^2, \\ \mathbf{k}_T &= \mathbf{P}_T, \end{aligned} \quad (3.4)$$

where  $k = (e, \mathbf{k}_T, k_z) = (e, k_x, k_y, k_z)$  contains the unknowns of the system, and  $p = (E, \mathbf{p}_T, p_z) = (E, p_x, p_y, p_z)$  is the visible particle momentum of the given collider event. Using the lexicographic ordering  $k_x \succ k_y \succ k_z \succ e$ , we find that the Gröbner basis of the system is given by

$$\begin{aligned} g_1 &= k_x - \mathbf{P}_x, \\ g_2 &= k_y - \mathbf{P}_y, \\ g_3 &= -2p_z k_z + 2Ee - (M_Y^2 - M_\chi^2 - m^2 + 2\mathbf{p}_T \cdot \mathbf{P}_T), \\ g_4 &= -4(E^2 - p_z^2)e^2 + 4E(M_Y^2 - M_\chi^2 - m^2 + 2\mathbf{p}_T \cdot \mathbf{P}_T)e \\ &\quad - (M_Y^2 - M_\chi^2 - m^2 + 2\mathbf{p}_T \cdot \mathbf{P}_T)^2 - 4p_z^2(M_\chi^2 + \|\mathbf{P}_T\|^2), \end{aligned} \quad (3.5)$$

where  $m^2 = p^2$ . We have four constraint equations and four unknowns. Therefore, the Jacobian is a  $4 \times 4$  matrix given as follows:

$$J_{ij} = \frac{\partial g_i}{\partial k_j} = \begin{pmatrix} 1 & & & \\ & 1 & & \\ & -2p_z & & 2E \\ & & -8(E^2 - p_z^2)e + 4E(M_Y^2 - M_\chi^2 - m^2 + 2\mathbf{p}_T \cdot \mathbf{P}_T) & \end{pmatrix}. \quad (3.6)$$

As mentioned earlier, taking the Gröbner basis renders the Jacobian matrix having the row echelon form. Except for the soft singularity where  $p_z = 0$ , the reduced rank condition requires the fourth diagonal term of  $J$  to be vanishing,

$$0 = J_{44} = 8p_z E e \left( \frac{p_z}{E} - \frac{k_z}{e} \right). \quad (3.7)$$

Here, we have used the constraints in (3.4) to eliminate  $M_Y^2$  and  $\mathbf{P}_T$ . Note that Eq. (3.7) is equivalent to the relation that

$$\frac{p_z}{E_T} = \frac{k_z}{e_T} \quad (3.8)$$

if  $p_z$ ,  $E$ , and  $e$  are all nonzero. By using the relation, we get

$$M_Y^2 = m^2 + M_\chi^2 + 2(E_T e_T - \mathbf{p}_T \cdot \mathbf{k}_T), \quad (3.9)$$

where  $\mathbf{k}_T = \mathbf{P}_T$ . The expression on the right-hand side is nothing but the transverse mass squared for the  $v$  and  $\chi$  system. It shows that the transverse mass corresponds to the singularity variable of the decay topology (3.3), as shown in Refs. [17–19, 24]. The transverse mass is the invariant mass in the  $(1+2)$ -dimensional space, and the algebraic singularity method tells us that it is an optimized variable. The Jacobian peak in the transverse mass distribution is indeed a feature of singularity.

### 3.1 Singularity variable for double-sided decay topology

After having recapitulated the  $M_{T2}$  variable and the algebraic singularity method, we now derive the singularity variable for double-sided decay topology. The investigation of its relation with the  $M_{T2}$  variable is presented in the following section. To derive the singularity variable using the algebraic singularity method, we should first identify all the kinematic constraint equations and the corresponding Gröbner basis. For the double-sided decay topology in (2.1), the kinematic constraints are given as follows:<sup>2</sup>

$$\begin{aligned} k_1^2 &= M_\chi^2, \\ k_2^2 &= M_\chi^2, \\ (p_1 + k_1)^2 &= M_Y^2, \\ (p_2 + k_2)^2 &= M_Y^2, \\ \mathbf{k}_{1T} + \mathbf{k}_{2T} &= \mathbf{P}_T. \end{aligned} \quad (3.10)$$

In this system, we have eight unknowns from the energy-momentum components of invisible particle momenta  $k_1$  and  $k_2$ , while there are six constraints from (3.10). Therefore, the system is underconstrained, and we need additional constraints or ansatz to solve the system. In the  $M_{T2}$  variable, the limitation has been overcome by the minimization over  $\mathbf{k}_{1T}$ , for a guessed value of  $M_\chi$ . In the algebraic singularity method, we will see that the reduced rank condition provides additional constraints to the unknowns. Note that the number of additional constraints furnished by the reduced rank condition depends on the form of diagonal components of the Jacobian matrix. As can be seen in the Jacobian matrix given in Eq. (3.6) and the matrix for the double-sided decay topology, which will be shown shortly, not all diagonal components of the Jacobian matrices can be set to be zero. Unless we find a theorem concerning the relation among the leading terms of Gröbner basis elements and decay topologies, it can be deduced only by explicitly obtaining the Gröbner basis of the polynomial equations of the given process. Therefore, it

---

<sup>2</sup>In the presence of multiple visible particles, the construction of kinematic constraints can be vulnerable to the combinatorial ambiguities on how to group the visible particles into separate sets. For instance, in the process of pair-produced gluinos decaying into jets,  $\tilde{g}\tilde{g} \rightarrow jj\tilde{\chi}_1^0 + jj\tilde{\chi}_1^0$  with  $j$  being a quark jet, there are three distinct ways of grouping the jets into two pairs of visible systems. We assume that the combinatorial ambiguity has been resolved by employing dedicated methods such as those proposed in Refs. [45–50].

is generally unclear whether the reduced rank condition for a given decay topology would always provide additional constraints enough to solve all the unknowns in conjunction with the known kinematic constraints. Nonetheless, we will see that we can obtain the constraints enough to solve the unknowns for an input mass  $M_\chi$  by using the reduced rank condition in the case of the double-sided decay topology.

As we have done in Sec. 2, we eliminate  $\mathbf{k}_{2T}$  by using the condition of missing transverse momentum. Then, we have four constraints from the on-shell mass relations and six unknowns. With the lexicographic ordering  $e_1 \succ e_2 \succ k_{1z} \succ k_{2z} \succ k_{1x} \succ k_{1y}$ , the Gröbner basis is given by

$$\begin{aligned}
g_1 &= 2E_1 e_1 - 2p_{1z} k_{1z} - 2p_{1x} k_{1x} - 2p_{1y} k_{1y} - (M_Y^2 - M_\chi^2 - m_1^2), \\
g_2 &= 2E_2 e_2 - 2p_{2z} k_{2z} + 2p_{2x} k_{1x} + 2p_{2y} k_{1y} - (M_Y^2 - M_\chi^2 - m_2^2 + 2\mathbf{p}_{2T} \cdot \mathbf{P}_T), \\
g_3 &= -4(E_1^2 - p_{1z}^2) k_{1z}^2 + 8p_{1x} p_{1z} k_{1z} k_{1x} + 8p_{1y} p_{1z} k_{1z} k_{1y} \\
&\quad + 4(M_Y^2 - M_\chi^2 - m_1^2) p_{1z} k_{1z} \\
&\quad - 4(E_1^2 - p_{1x}^2) k_{1x}^2 + 8p_{1x} p_{1y} k_{1x} k_{1y} \\
&\quad + 4(M_Y^2 - M_\chi^2 - m_1^2) p_{1x} k_{1x} \\
&\quad - 4(E_1^2 - p_{1y}^2) k_{1y}^2 + 4(M_Y^2 - M_\chi^2 - m_1^2) p_{1y} k_{1y} \\
&\quad + (M_Y^2 - M_\chi^2 - m_1^2)^2 - 4E_1^2 M_\chi^2, \\
g_4 &= -4(E_2^2 - p_{2z}^2) k_{2z}^2 - 8p_{2x} p_{2z} k_{2z} k_{1x} - 8p_{2y} p_{2z} k_{2z} k_{1y} \\
&\quad + 4(M_Y^2 - M_\chi^2 - m_2^2 + 2\mathbf{p}_{2T} \cdot \mathbf{P}_T) p_{2z} k_{2z} \\
&\quad - 4(E_2^2 - p_{2x}^2) k_{1x}^2 + 8p_{2x} p_{2y} k_{1x} k_{1y} \\
&\quad - 4[(M_Y^2 - M_\chi^2 - m_2^2 + 2\mathbf{p}_{2T} \cdot \mathbf{P}_T) p_{2x} - 2E_2^2 \mathcal{P}_x] k_{1x} \\
&\quad - 4(E_2^2 - p_{2y}^2) k_{1y}^2 - 4[(M_Y^2 - M_\chi^2 - m_2^2 + 2\mathbf{p}_{2T} \cdot \mathbf{P}_T) p_{2y} - 2E_2^2 \mathcal{P}_y] k_{1y} \\
&\quad + (M_Y^2 - M_\chi^2 - m_2^2 + 2\mathbf{p}_{2T} \cdot \mathbf{P}_T)^2 - 4E_2^2 (M_\chi^2 + \|\mathbf{P}_T\|^2). \tag{3.11}
\end{aligned}$$

Hypothesizing the values of  $M_Y$  and  $M_\chi$ , we can solve the polynomial equations to obtain the solution to the unknowns for a given  $\mathbf{k}_{1T} = (k_{1x}, k_{1y})$ . The expressions of the solutions of  $g_i$  are given as follows:

$$\begin{aligned}
e_a &= \frac{A_a + p_{az} k_{az}}{E_a}, \\
k_{az} &= \frac{p_{az} A_a \pm E_a \sqrt{A_a^2 - E_{aT}^2 e_{aT}^2}}{E_{aT}^2}, \tag{3.12}
\end{aligned}$$

and  $\mathbf{k}_{2T} = \mathbf{P}_T - \mathbf{k}_{1T}$ . Here,

$$A_a = \frac{M_Y^2 - M_\chi^2 - m_a^2}{2} + \mathbf{p}_{aT} \cdot \mathbf{k}_{aT} \tag{3.13}$$

is the same as that defined in Ref. [10]. Due to the quadratic equations  $g_3$  and  $g_4$ , we have two degenerate solutions for each longitudinal component.

The Jacobian matrix of the Gröbner basis is the  $4 \times 6$  matrix given by

$$J = \begin{pmatrix} 2E_1 & & -2p_{1z} & & -2p_{1x} & -2p_{1y} \\ & 2E_2 & & -2p_{2z} & 2p_{2x} & 2p_{2y} \\ & & \partial g_3 / \partial k_{1z} & & \partial g_3 / \partial k_{1x} & \partial g_3 / \partial k_{1y} \\ & & & \partial g_4 / \partial k_{2z} & \partial g_4 / \partial k_{1x} & \partial g_4 / \partial k_{1y} \end{pmatrix}, \tag{3.14}$$

where

$$\begin{aligned}
\frac{\partial g_3}{\partial k_{1z}} &= 8p_{1z}(A_1 + p_{1z}k_{1z}) - 8E_1^2 k_{1z}, \\
\frac{\partial g_3}{\partial k_{1x}} &= 8p_{1x}(A_1 + p_{1z}k_{1z}) - 8E_1^2 k_{1x}, \\
\frac{\partial g_3}{\partial k_{1y}} &= 8p_{1y}(A_1 + p_{1z}k_{1z}) - 8E_1^2 k_{1y}, \\
\frac{\partial g_4}{\partial k_{2z}} &= 8p_{2z}(A_2 + p_{2z}k_{2z}) - 8E_2^2 k_{2z}, \\
\frac{\partial g_4}{\partial k_{1x}} &= -8p_{2x}(A_2 + p_{2z}k_{2z}) + 8E_2^2 (\not{P}_x - k_{1x}), \\
\frac{\partial g_4}{\partial k_{1y}} &= -8p_{2y}(A_2 + p_{2z}k_{2z}) + 8E_2^2 (\not{P}_y - k_{1y}).
\end{aligned} \tag{3.15}$$

Except for the soft singularities where  $E_1 = 0$  and  $E_2 = 0$ , the reduced rank condition for the Jacobian matrix in Eq. (3.14) implies that

$$\frac{\partial g_3}{\partial k_{1z}} = 0, \tag{3.16}$$

$$\frac{\partial g_4}{\partial k_{2z}} = 0, \tag{3.17}$$

$$\det \begin{pmatrix} \partial g_3 / \partial k_{1x} & \partial g_3 / \partial k_{1y} \\ \partial g_4 / \partial k_{1x} & \partial g_4 / \partial k_{1y} \end{pmatrix} = 0. \tag{3.18}$$

Note that from the vanishing diagonal terms, i.e., Eqs. (3.16) and (3.17), each longitudinal component is uniquely determined as

$$k_{az} = \frac{p_{az}A_a}{E_{aT}^2}. \tag{3.19}$$

The expressions of the longitudinal momenta are the same as in the modified MAOS method proposed in Ref. [51]. By comparing the longitudinal components with those in Eq. (3.12), we find that the condition of vanishing diagonal terms is equivalent to

$$A_a = E_{aT}e_{aT}. \tag{3.20}$$

From the definition of  $A_a$  given in Eq. (3.13), the first two of the above conditions turn out to be

$$\begin{aligned}
M_Y^2 &= m_1^2 + M_\chi^2 + 2(E_{1T}e_{1T} - \mathbf{p}_{1T} \cdot \mathbf{k}_{1T}), \\
M_Y^2 &= m_2^2 + M_\chi^2 + 2(E_{2T}e_{2T} - \mathbf{p}_{2T} \cdot \mathbf{k}_{2T}),
\end{aligned} \tag{3.21}$$

which are the transverse masses of  $v_1\chi$  and  $v_2\bar{\chi}$  systems. Interestingly, we have arrived at a similar conclusion as in the previous discussion: the transverse masses are the singularity variables of the double-sided decay topology where there exists an invisible particle in each decay chain. Because we here consider symmetric decay chains, the condition (3.21) corresponds to the balanced configuration, where

$$M_{1T} = M_{2T}. \tag{3.22}$$

Because  $\mathbf{k}_{2T} = \mathbf{P}_T - \mathbf{k}_{1T}$ , this condition is an equation of two variables,  $k_{1x}$  and  $k_{1y}$ .

The condition (3.18) is a new one that does not appear in the derivation of the singularity variable for single-sided decay topology. After eliminating  $M_Y^2$  using  $A_1$  in  $\partial g_3/\partial \mathbf{k}_{1T}$  and using  $A_2$  in  $\partial g_4/\partial \mathbf{k}_{1T}$ , then substituting the singularity solutions into the invisible longitudinal momenta given in (3.19), we get

$$\det \begin{pmatrix} \partial g_3/\partial k_{1x} & \partial g_3/\partial k_{1y} \\ \partial g_4/\partial k_{1x} & \partial g_4/\partial k_{1y} \end{pmatrix} = \frac{64E_1^2 E_2^2}{E_{1T}^2 E_{2T}^2} \det \begin{pmatrix} A_1 p_{1x} - E_{1T}^2 k_{1x} & A_1 p_{1y} - E_{1T}^2 k_{1y} \\ -A_2 p_{2x} + E_{2T}^2 (\mathbf{P}_x - k_{1x}) & -A_2 p_{2y} + E_{2T}^2 (\mathbf{P}_y - k_{1y}) \end{pmatrix}. \quad (3.23)$$

Then, by using the condition in (3.20), we arrive at

$$0 = \det \begin{pmatrix} \partial g_3/\partial k_{1x} & \partial g_3/\partial k_{1y} \\ \partial g_4/\partial k_{1x} & \partial g_4/\partial k_{1y} \end{pmatrix} = \frac{16E_1^2 E_2^2 e_{1T} e_{2T}}{E_{1T} E_{2T}} \det \begin{pmatrix} \partial M_{1T}^2/\partial k_{1x} & \partial M_{1T}^2/\partial k_{1y} \\ \partial M_{2T}^2/\partial k_{1x} & \partial M_{2T}^2/\partial k_{1y} \end{pmatrix}, \quad (3.24)$$

where we have used the expressions of the gradients of the transverse masses given in (2.11). If all the transverse energies  $E_{aT}$  and  $e_{aT}$  are nonzero, the reduced rank condition implies that the determinant of the Jacobian matrix for the transverse masses is vanishing at singularities.

Summarizing our findings so far, the reduced rank condition for the double-sided decay topology has led to two conditions at singularity points:

- (i) the balanced configuration of the transverse masses, Eq. (3.22),
- (ii) and the vanishing determinant of the Jacobian matrix for the transverse masses, Eq. (3.24).

Because the conditions provide two equations, we can solve them to obtain the unknowns,  $k_{1x}$  and  $k_{1y}$ , for trial mass  $M_\chi$ .<sup>3</sup> This is in contrast with the  $M_{T2}$  variable, which is obtained by the minimization of the objective function (2.7) over  $k_{1x}$  and  $k_{1y}$ .

## 4 Comparison of $M_{T2}$ and singularity variables

We are now in a position to examine the singularity variable of double-sided decay topology by comparing it with the  $M_{T2}$  variable. As we have seen in Sec. 2, the convexity of the  $M_{T2}$  objective function ensures that the global minimum of the objective function and the corresponding solutions to the transverse momenta of the invisible particles are uniquely determined for each event. On the other hand, Eqs. (3.22) and (3.24) are a coupled nonlinear system, which may yield multiple solutions to the invisible particle momenta. As a

---

<sup>3</sup>For asymmetric decay chains, that is,  $M_Y \neq M_{\bar{Y}}$ , the reduced rank condition gives us three equations, two from the transverse masses and one from the vanishing determinant of the Jacobian matrix. The system is underconstrained unless we have ansatz for either  $M_Y$  or  $M_{\bar{Y}}$ .

result of the minimization, the endpoint of the  $M_{T2}$  distribution is smaller than or equal to the parent particle, as in Eq. (2.6). The reduced rank condition, however, does not warrant such a feature on the singularity variables. Moreover, it is challenging to solve Eqs. (3.22) and (3.24) analytically by transforming or reducing it to a simpler form. It is not even clear to see if the solution of the equations would be unique. Therefore, we rely on sequential numerical methods to obtain the solutions of the equations.

Because both  $M_{T2}$  and singularity variables do not have analytic expressions in general cases, the comparison of the two different types of variables is not a straightforward task. If either or both of  $\partial M_{1T}/\partial \mathbf{k}_{1T}$  and  $\partial M_{2T}/\partial \mathbf{k}_{1T}$  are vanishing, the condition (3.24) is trivially satisfied, but it does not always lead to the balanced configuration,  $M_{1T} = M_{2T}$ . In the case where visible particle systems are massless and upstream momentum is vanishing, we have seen that the  $M_{T2}$  solution to the invisible particle momenta in balanced configurations is given by Eq. (2.18). Indeed, when  $m_1 = m_2 = 0$ , the condition (2.14) always holds, and thus every collider event is in a balanced configuration. One can see that the analytic expression of the  $M_{T2}$  solution (2.18) satisfies both conditions, Eqs. (3.22) and (3.24). Therefore, in this particular case, we have proven that the singularity variables *contain* the  $M_{T2}$  variable.

For comparing the two types of collider variables, we have generated one million phase-space event sample and calculated the variables by employing numerical algorithms. As our study concentrates on the pure comparison of the  $M_{T2}$  and singularity variables, we do not take into account realistic detector effects, such as particle momentum smearing and misidentification rates, in our simulation. For calculating  $M_{T2}$ , we used the public software package based on the bisection method [52]. As we are not aware of any software package for singularity variables, we have calculated them by using our own code implementation. As noted earlier, Eq. (3.24) is not the polynomial equation of  $\mathbf{k}_{1T}$ , and it can possess multiple real or complex solutions. To solve Eqs. (3.22) and (3.24), we repeat Newton's method with a large number of heuristically chosen initial guesses for  $\mathbf{k}_{1T}$  in our code implementation. For a cross-check, we have compared the results from our code with those from the `NSolve` method of `Mathematica`<sup>TM</sup>, which can find multiple roots of nonlinear equations. We will release our code implementation for calculating the singularity variables as a public software package in a separate publication.

In Fig. 2, we display the distributions of the singularity and the  $M_{T2}$  variables for phase-space events of  $M_Y = 500$  GeV and  $M_\chi = 200$  GeV. The visible particle systems are taken to be massless. In the figure,  $M_{\text{SG}}$  denotes the singularity variables in (3.21), i.e.,

$$M_{\text{SG}} = M_{1T} = M_{2T} = \frac{M_{1T} + M_{2T}}{2}. \quad (4.1)$$

When there exist multiple solutions for invisible particle momenta in an event, we will have multiple values of  $M_{\text{SG}}$ . In this case, we can take the minimum and the maximum among the  $M_{\text{SG}}$  values into separate consideration,

$$M_{\text{SG}}^{\min} \leq M_{\text{SG}} \leq M_{\text{SG}}^{\max}. \quad (4.2)$$

If  $M_{\text{SG}}$  were invariant masses, the parent particle mass  $M_Y$  would be bounded as  $M_{\text{SG}}^{\min} \leq M_Y \leq M_{\text{SG}}^{\max}$ , as in the case of the antler decay topology studied in Refs. [19,20]. However,



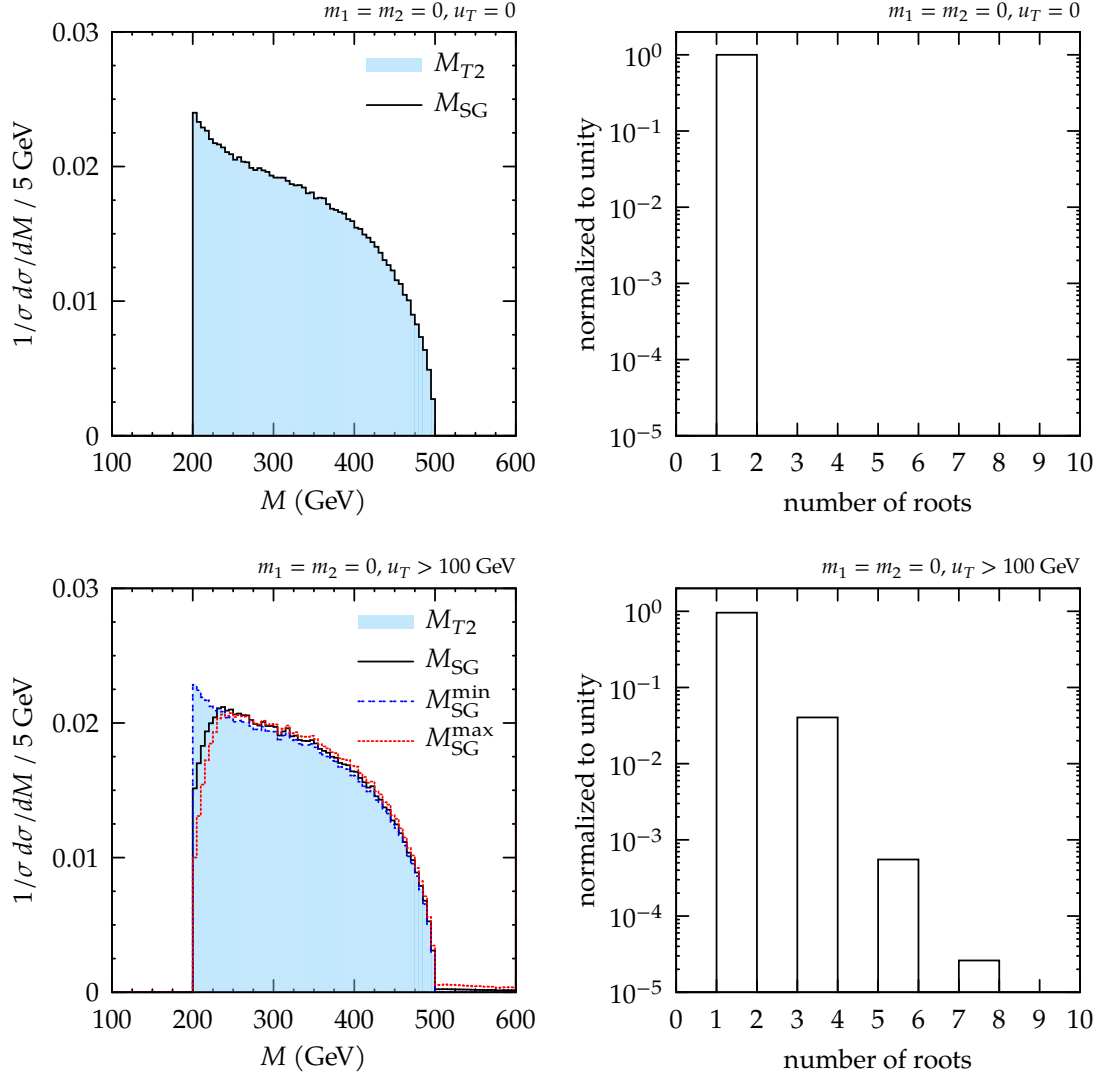


Figure 2: Distributions of the singularity variables  $M_{\text{SG}}$  and  $M_{T2}$  (left) and the number of roots of reduced rank conditions (right) for phase-space events of  $M_Y = 500$  GeV and  $M_\chi = 200$  GeV. In the upper panels, the upstream momentum  $u_T$  is vanishing, while in the lower panels, it is larger than 100 GeV. The visible particle systems are all massless,  $m_1 = m_2 = 0$ , and we have taken  $M_\chi = M_\chi^{\text{true}}$ .

the mass hierarchy does not hold because both  $M_{\text{SG}}^{\text{min}}$  and  $M_{\text{SG}}^{\text{max}}$  could be smaller than  $M_Y$  for  $M_{\text{SG}}$  being transverse masses. In the upper panels of Fig. 2, we show the distributions in the case of vanishing upstream momentum. As already noted, in this case, the  $M_{T2}$  solution to the invisible particle momenta satisfies the reduced rank condition of the algebraic singularity method. Thus, one might expect that one of the  $M_{\text{SG}}$  values would be in accord with the  $M_{T2}$  value while the others would have different values. Our numerical study shows that the singularity solution to the invisible particle momenta is unique for all events and  $M_{T2} = M_{\text{SG}}$ . We conjecture that this observation led the author of Ref. [15] to a conclusion: “the  $M_{T2}$  variable could be derived from the algebraic singularity method.” However, to arrive at the right conclusion, we should also investigate the more general



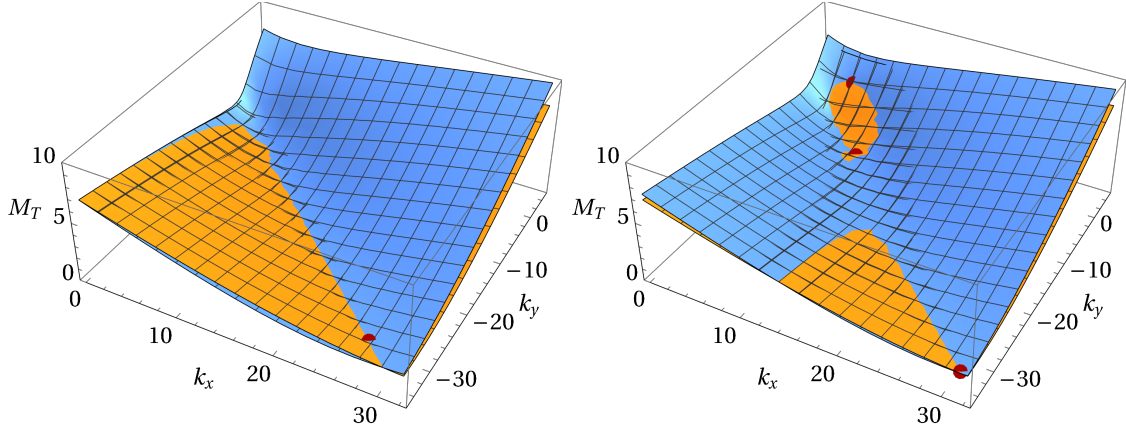


Figure 3: Transverse masses  $M_{1T}$  and  $M_{2T}$  for an event with vanishing (left) and nonvanishing upstream momentum (right). The red points in each plot correspond to the solutions to the reduced rank condition of the algebraic singularity method. The scales of axes are arbitrarily normalized.

cases with nonvanishing upstream momentum and nonzero visible particle masses. The distributions for events with large upstream momentum  $u_T > 100$  GeV are shown in the lower panels of Fig. 2. In this case, we find that there exist events with multiple solutions, although a vast majority of events possess unique solutions to the reduced rank condition. In the  $M_{\text{SG}}$  distribution, we have appropriately weighted the histogram for the events having multiple solutions. We observe that even if multiple solutions exist, the minimum among the  $M_{\text{SG}}$  values is still identical to the  $M_{T2}$  value, i.e.,

$$M_{\text{SG}} \geq M_{T2} \quad (4.3)$$

for all events. It implies that some of the  $M_{\text{SG}}$  values can exceed the true parent particle mass  $M_Y^{\text{true}}$  because the  $M_{T2}$  distribution is bounded from above by  $M_Y^{\text{true}}$  for  $M_\chi = M_\chi^{\text{true}}$ . However, the rate of events with  $M_{\text{SG}} > M_Y^{\text{true}}$  is quite small, as can be seen in the lower left panel of Fig. 2.

We lack the understanding of the condition for having multiple solutions to the reduced rank condition unless we find the analytic expressions of the solutions to Eqs. (3.22) and (3.24). Still, we may acquire a rough understanding of the multiple solutions by looking at the shapes of the transverse mass functions in the presence of upstream momentum. In Fig. 3, we show the transverse masses in the space of  $(k_{1x}, k_{1y})$  for an event with vanishing or nonvanishing upstream momentum. In the case where upstream momentum is vanishing, the points of balanced configurations  $M_{1T} = M_{2T}$  lie on a connected curve. Among the points on the curve, the iterations of the  $M_{T2}$  calculation will stop at a point that gives the minimum of the objective function (2.7). In the singularity method, we alternatively look for points satisfying the vanishing determinant condition (3.24). We have found that the two different methods pick out an identical point when upstream momentum is vanishing. See the left panel of Fig. 3. On the other hand, if upstream momentum is nonvanishing, the curves of balanced configuration can appear in disconnected regions in the space of invisible particle momentum. The  $M_{T2}$  variable will still

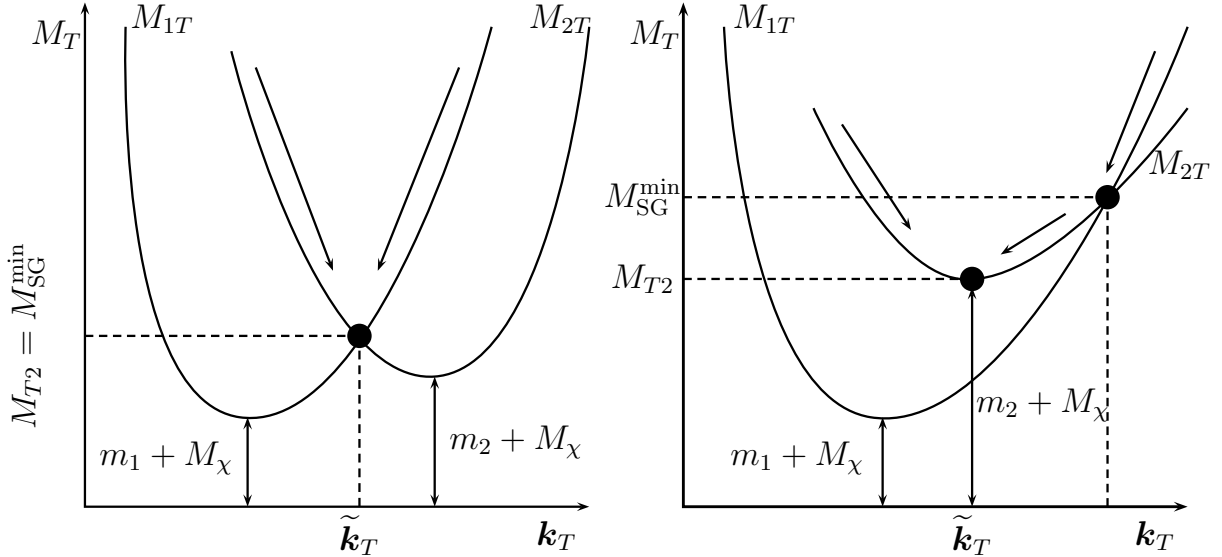


Figure 4: The same pictures as in Fig. 1, but with depicting the minimum value of the singularity variable  $M_{SG}^{\min}$ . The black dots in each plot correspond to either or both of the  $M_{T2}$  and the  $M_{SG}^{\min}$  values.  $\tilde{k}_T$  denotes the  $M_{T2}$  solution to the invisible particle momenta.

take one point among them, where the objective function is minimized, whereas several points on different curves can satisfy the reduced rank condition, as can be seen in the right panel of Fig. 3. In this situation, we will have multiple solutions in the algebraic singularity method. Our numerical study shows that one of the multiple solutions is still identical to the point picked out by the  $M_{T2}$  variable in balanced configurations. We note that the physical interpretation of the multiple solutions to the reduced rank condition is still unknown, and we are in eager pursuit of new insights into the better understanding of the multiple solutions.

We now turn our attention to the case of massive visible particle systems. We have generated separate phase-space event sample while keeping the  $M_Y$  and  $M_X$  values unchanged. Now, the masses of the visible particle system,  $m_1$  and  $m_2$ , are set to be varying between 0 and  $M_Y - M_X$  as in the three-body decay process. A notable difference in comparison to the massless case is the presence of unbalanced configurations. Recall that unbalanced configurations where  $M_{1T} \neq M_{2T}$  occur when the condition (2.14) does not hold. About 35% of our event sample is in unbalanced configurations. In such events, the  $M_{T2}$  solution can never satisfy the reduced rank condition because it violates the condition in Eq. (3.22). On the other hand, in the case of balanced configuration, we can expect the same relation as in the massless case. The locations of  $M_{SG}^{\min}$  in two different configurations are depicted in Fig. 4. The right panel of Fig. 4 shows that  $M_{SG}^{\min}$  can be larger than the  $M_{T2}$  value in unbalanced configurations. There is another case the figure does not show: the singularity variable goes *undefined* if the collider event is in an unbalanced configuration and the transverse masses never meet at any point in the physical domain of  $\mathbf{k}_{1T}$ . Even in this case, the  $M_{T2}$  value is given by either of the stationary points of  $M_{1T}$  and  $M_{2T}$ .

The  $M_{T2}$  and the  $M_{SG}$  distributions for phase-space event data with massive visible

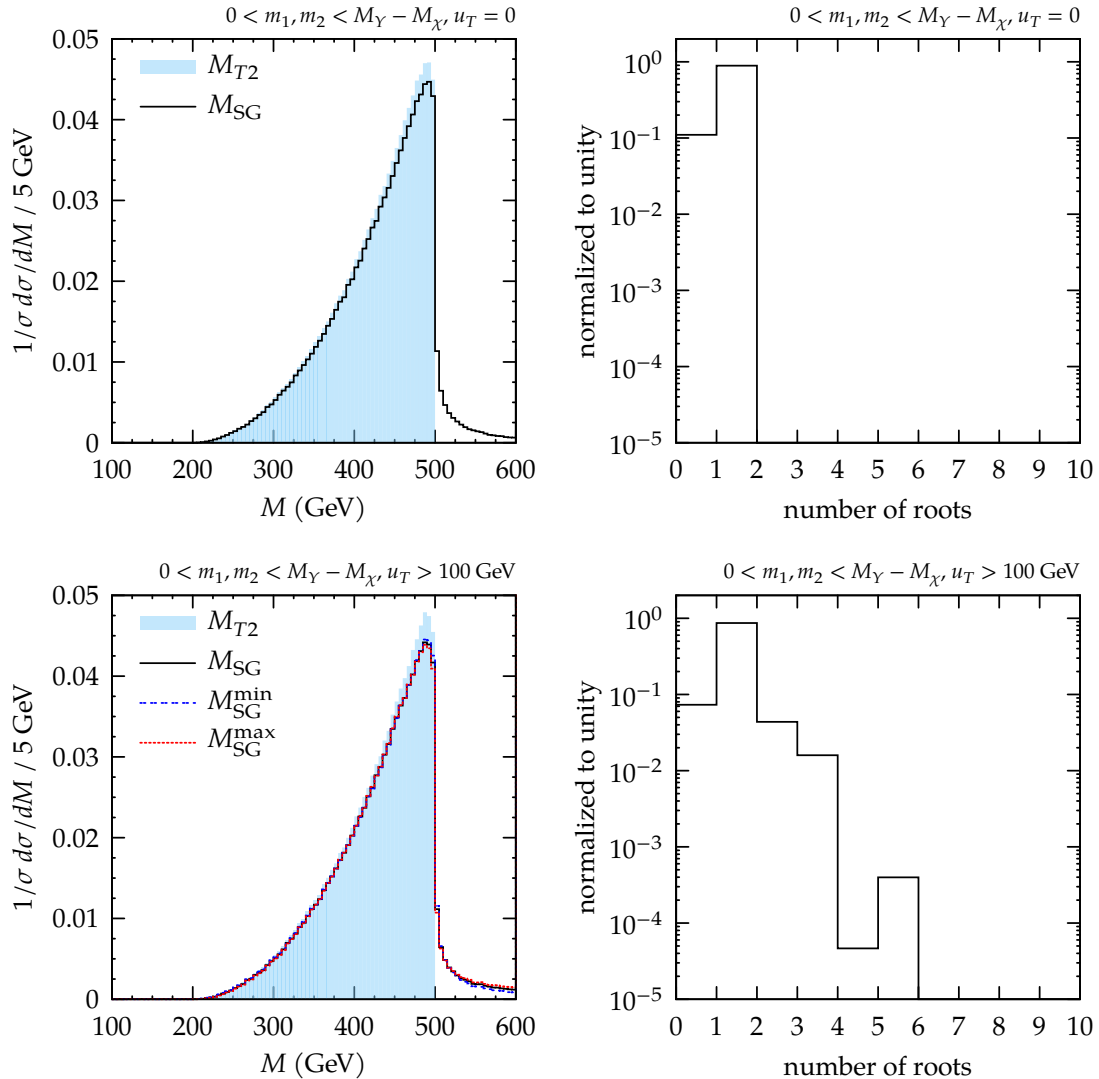


Figure 5: Distributions of the singularity variables  $M_{\text{SG}}$  and  $M_{T2}$  (left) and the number of roots of reduced rank conditions (right) for phase-space events of  $M_Y = 500$  GeV and  $M_\chi = 200$  GeV. The masses of visible particle systems are varying between 0 and  $M_Y - M_\chi$ , and we have taken  $M_\chi = M_\chi^{\text{true}}$ . In the upper panels, the upstream momentum  $u_T$  is vanishing, while in the lower panels, it is larger than 100 GeV.

particles are shown in Fig. 5. We find that the singularity variable is undefined for about 10% of events.<sup>4</sup> For comparison, we show the distributions for the events where the singularity variable can be attained. As in the case of massless visible particle systems, the singularity variable is uniquely determined when upstream momentum is vanishing. However, due to the presence of unbalanced configurations, the endpoint of the  $M_{\text{SG}}$  distribution exceeds the parent particle mass  $M_Y$ , as can be seen in the upper left panel

<sup>4</sup>One way of resolving the problem of undefined singularity variable is to relax the condition of balanced configuration (3.22). We may use the minimum of  $|M_{1T} - M_{2T}|$  (or  $(M_{1T} - M_{2T})^2$ ) subject to the condition of vanishing determinant in (3.24). We have implemented the modified singularity variable in our numerical study and found it is identical to  $M_{T2}$ .

of Fig. 5. On the other hand, the reduced rank condition can yield multiple solutions in the case where upstream momentum is nonvanishing, even though most of the events still possess unique solutions. In both cases, we observe that the  $M_{\text{SG}}$  distributions have a sharp peak around the parent particle mass. Therefore, we expect that the singularity variable can be useful for the discovery or the mass measurement of new particles at collider experiments.

## 4.1 Beyond trivial zero

We finally consider an interesting case where the visible and the invisible particles are all massless,  $m_1 = m_2 = M_\chi = 0$ . We often deal with the fully massless case in both Standard Model (SM) measurements and new physics searches. For example, in the  $WW \rightarrow \ell^+ \nu \ell^- \bar{\nu}$  process, which we will investigate in this subsection, all the final-state particles are massless. In the searches for supersymmetric processes, e.g., pair produced sleptons decaying to charged leptons and the lightest neutralinos, the final-state particles are often assumed to be massless in the simplified model approach. See, for instance, Refs. [53, 54].

In Sec. 2, we have seen that the  $M_{T2}$  solution to invisible particle momenta would simply be given by Eq. (2.21) when upstream momentum is vanishing. In the case of nonzero upstream momentum, the missing transverse momentum  $\mathbf{P}_T$  may lie inside the smaller sector bounded by visible particle momenta  $\mathbf{p}_{1T}$  and  $\mathbf{p}_{2T}$ . In this situation, the  $M_{T2}$  value is zero because the invisible momenta is taken to be  $\mathbf{k}_{aT} \propto \mathbf{p}_{aT}$ . This is called a *trivial zero* of  $M_{T2}$  [34]. It is not a coincidence but an unexpected consequence of minimization inherent to the definition of  $M_{T2}$ .

To investigate the trivial zero of  $M_{T2}$ , we have generated Monte Carlo event samples of the dileptonic top pair process by using `Pythia` [55]. The proton-proton collision energy has been set to be 13 TeV. We take the  $WW$  subsystem of the top-pair decay events, so the upstream momentum is given by  $\mathbf{u}_T = \mathbf{p}_T^b + \mathbf{p}_T^{\bar{b}}$  plus the transverse momentum of initial state radiations. The distributions of  $M_{T2}$  and  $M_{\text{SG}}^{\text{max}}$  are shown in Fig. 6. For the  $WW$  subsystem, every event is in a balanced configuration. Therefore,  $M_{\text{SG}}^{\text{min}} = M_{T2}$  for all events. The  $M_{T2}$  distribution has a peak around  $M_{T2} = 0$ , which is due to the trivial zero of  $M_{T2}$ . Meanwhile, the  $M_{\text{SG}}^{\text{max}}$  distribution does not have a peak at zero, and it has a smoothly-falling shape around the  $W$  boson mass. Consequently, the  $M_{\text{SG}}^{\text{max}}$  distribution has a more number of events around the  $W$  boson mass than the  $M_{T2}$  distribution, as can be seen in the insert plot in Fig. 6.

From this observation, we expect that using the  $M_{\text{SG}}^{\text{max}}$  distribution in the fully massless case could be more advantageous than  $M_{T2}$  in the situation where the trivial zero of  $M_{T2}$  affects the statistical significance of new physics searches. For instance, if one takes the lightest neutralino mass to be zero, many signal events of the slepton pair process will have the  $M_{T2}$  value at zero, and one of the dominant backgrounds, the SM  $WW + \text{jet}$  process, will also have a high population in the same bin. It can be circumvented by using  $M_{\text{SG}}^{\text{max}}$ , which is free from trivial zero, and its distribution has an edge around the hypothesized slepton mass.

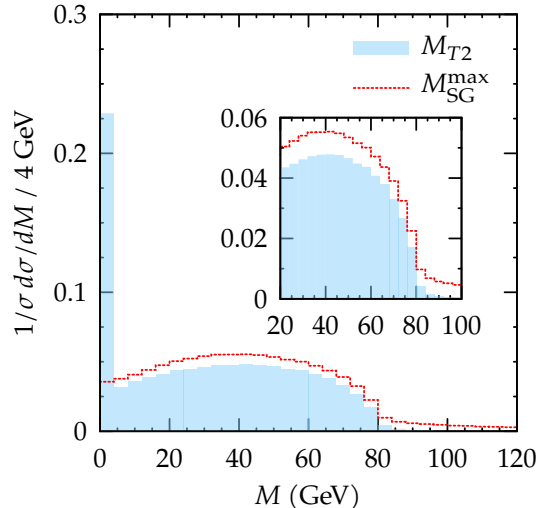


Figure 6: Distributions of  $M_{T2}$  and  $M_{SG}^{\max}$  in the  $WW$  subsystem of top pair process. The insert in the plot shows the distributions in the mass region between 20 and 100 GeV.

## 5 Conclusions

The  $M_{T2}$  variable is served as the observable of choice when analyzing the collider events of double-sided decay topology with invisible particles in the final state. Meanwhile, the algebraic singularity method is still less studied compared to the  $M_{T2}$  variable. It is a framework for studying any decay topology containing invisible particles by exploiting all the available kinematic constraints. We can derive singularity variables from the reduced rank condition of the algebraic singularity method. The singularity variables are supposed to be optimal because they can capture singular features characteristic to the decay topology under consideration.

The question investigated in this article is whether the  $M_{T2}$  variable is also a singularity variable, or we can derive another kinematic variables more optimal than the  $M_{T2}$  by applying the algebraic singularity method to the double-sided decay topology. The analytic comparison of the  $M_{T2}$  variable and the corresponding singularity variable is challenging because their analytic expressions are not available yet. However, in some special cases, e.g., when the visible particle systems are massless and upstream momentum is vanishing, we have found that the  $M_{T2}$  variable is in accord with the singularity variable  $M_{SG}$ . In the other cases, multiple singularity solutions can exist, and we demonstrated that the  $M_{T2}$  variable is still contained in the singularity variables in many cases. Indeed, it corresponds to the minimum of the singularity variables,  $M_{T2} \leq M_{SG}$ , except for the unbalanced configurations of  $M_{T2}$ . In the latter case, the  $M_{T2}$  value can be distinct from the singularity variables. We hope that this article would serve as supplementary material for studying the algebraic singularity method.

The singularity variables can also be compared with another type of kinematic variables,  $M_2$ , which is an extension of  $M_{T2}$  to the  $(1+3)$ -dimensional space [12]. The singularity coordinate has been derived in Ref. [19], but detailed analysis using the Gröbner

basis is missing. We will perform the analysis in our future publication.

Another aspect that has not been considered in this article is the effects of a realistic collider environment, such as particle momentum resolutions, misidentification rates, and combinatorial uncertainties in the presence of multiple visible particles. They should be properly examined for practical applications of the algebraic singularity method to physics analyses at colliders. We stress that the study deserves follow-up works for concrete physics processes, including realistic simulations with backgrounds.

## Acknowledgments

The author is grateful to Seodong Shin for valuable comments on the manuscript. This work was supported by Institute for Basic Science (IBS) under the project code, IBS-R018-D1.

## References

- [1] C. G. Lester and D. J. Summers, “Measuring masses of semiinvisibly decaying particles pair produced at hadron colliders,” *Phys. Lett. B* **463** (1999) 99–103, [arXiv:hep-ph/9906349](#).
- [2] A. Barr, C. Lester, and P. Stephens, “ $m_{T2}$ : The Truth behind the glamour,” *J. Phys. G* **29** (2003) 2343–2363, [arXiv:hep-ph/0304226](#).
- [3] W. S. Cho, K. Choi, Y. G. Kim, and C. B. Park, “Measuring the top quark mass with  $m_{T2}$  at the LHC,” *Phys. Rev. D* **78** (2008) 034019, [arXiv:0804.2185 \[hep-ph\]](#).
- [4] **CDF** Collaboration, T. Aaltonen *et al.*, “Measurement of the Top Quark Mass in the Dilepton Channel Using  $m_{T2}$  at CDF,” *Phys. Rev. D* **81** (2010) 031102, [arXiv:0911.2956 \[hep-ex\]](#).
- [5] D. Guadagnoli and C. B. Park, “ $M_{T2}$ -reconstructed invisible momenta as spin analyzers, and an application to top polarization,” *JHEP* **01** (2014) 030, [arXiv:1308.2226 \[hep-ph\]](#).
- [6] **CMS** Collaboration, A. M. Sirunyan *et al.*, “Measurement of the top quark mass in the dileptonic  $t\bar{t}$  decay channel using the mass observables  $M_{bl}$ ,  $M_{T2}$ , and  $M_{bl\nu}$  in pp collisions at  $\sqrt{s} = 8$  TeV,” *Phys. Rev. D* **96** no. 3, (2017) 032002, [arXiv:1704.06142 \[hep-ex\]](#).
- [7] A. J. Barr and C. Gwenlan, “The Race for supersymmetry: Using  $m_{T2}$  for discovery,” *Phys. Rev. D* **80** (2009) 074007, [arXiv:0907.2713 \[hep-ph\]](#).
- [8] **ATLAS** Collaboration, G. Aad *et al.*, “Search for new phenomena in events with two opposite-charge leptons, jets and missing transverse momentum in pp collisions

- at  $\sqrt{s} = 13$  TeV with the ATLAS detector,” *JHEP* **04** (2021) 165, [arXiv:2102.01444 \[hep-ex\]](#).
- [9] CMS Collaboration, A. Tumasyan *et al.*, “Search for electroweak production of charginos and neutralinos in proton-proton collisions at  $\sqrt{s} = 13$  TeV,” [arXiv:2106.14246 \[hep-ex\]](#).
- [10] W. S. Cho, K. Choi, Y. G. Kim, and C. B. Park, “ $M_{T2}$ -assisted on-shell reconstruction of missing momenta and its application to spin measurement at the LHC,” *Phys. Rev. D* **79** (2009) 031701, [arXiv:0810.4853 \[hep-ph\]](#).
- [11] W. S. Cho, J. E. Kim, and J.-H. Kim, “Amplification of endpoint structure for new particle mass measurement at the LHC,” *Phys. Rev. D* **81** (2010) 095010, [arXiv:0912.2354 \[hep-ph\]](#).
- [12] W. S. Cho, J. S. Gainer, D. Kim, K. T. Matchev, F. Moortgat, L. Pape, and M. Park, “On-shell constrained  $M_2$  variables with applications to mass measurements and topology disambiguation,” *JHEP* **08** (2014) 070, [arXiv:1401.1449 \[hep-ph\]](#).
- [13] V. D. Barger, A. D. Martin, and R. J. N. Phillips, “Perpendicular  $\nu_e$  Mass From  $W$  Decay,” *Z. Phys. C* **21** (1983) 99.
- [14] J. Smith, W. L. van Neerven, and J. A. M. Vermaseren, “The Transverse Mass and Width of the  $W$  Boson,” *Phys. Rev. Lett.* **50** (1983) 1738.
- [15] I.-W. Kim, “Algebraic Singularity Method for Mass Measurement with Missing Energy,” *Phys. Rev. Lett.* **104** (2010) 081601, [arXiv:0910.1149 \[hep-ph\]](#).
- [16] I.-W. Kim and C. B. Park. Private communication.
- [17] A. Rujula and A. Galindo, “Measuring the  $W$ -Boson mass at a hadron collider: a study of phase-space singularity methods,” *JHEP* **08** (2011) 023, [arXiv:1106.0396 \[hep-ph\]](#).
- [18] A. De Rujula and A. Galindo, “Singular ways to search for the Higgs boson,” *JHEP* **06** (2012) 091, [arXiv:1202.2552 \[hep-ph\]](#).
- [19] K. T. Matchev and P. Shyamsundar, “Singularity Variables for Missing Energy Event Kinematics,” *JHEP* **04** (2020) 027, [arXiv:1911.01913 \[hep-ph\]](#).
- [20] C. B. Park, “A singular way to search for heavy resonances in missing energy events,” *JHEP* **07** (2020) 089, [arXiv:2005.12297 \[hep-ph\]](#).
- [21] D. Kim, K. Kong, K. T. Matchev, M. Park, and P. Shyamsundar, “Deep-Learned Event Variables for Collider Phenomenology,” [arXiv:2105.10126 \[hep-ph\]](#).
- [22] H.-C. Cheng and Z. Han, “Minimal Kinematic Constraints and  $m_{T2}$ ,” *JHEP* **12** (2008) 063, [arXiv:0810.5178 \[hep-ph\]](#).



- [23] A. J. Barr, B. Gripaios, and C. G. Lester, “Transverse masses and kinematic constraints: from the boundary to the crease,” *JHEP* **11** (2009) 096, [arXiv:0908.3779 \[hep-ph\]](#).
- [24] **New Physics Working Group** Collaboration, G. Brooijmans *et al.*, “New Physics at the LHC. A Les Houches Report: Physics at TeV Colliders 2009 - New Physics Working Group,” in *6th Les Houches Workshop on Physics at TeV Colliders*, pp. 191–380. 5, 2010. [arXiv:1005.1229 \[hep-ph\]](#).
- [25] P. Agrawal, C. Kilic, C. White, and J.-H. Yu, “Improved Mass Measurement Using the Boundary of Many-Body Phase Space,” *Phys. Rev. D* **89** no. 1, (2014) 015021, [arXiv:1308.6560 \[hep-ph\]](#).
- [26] D. Debnath, J. S. Gainer, C. Kilic, D. Kim, K. T. Matchev, and Y.-P. Yang, “Enhancing the discovery prospects for SUSY-like decays with a forgotten kinematic variable,” *JHEP* **05** (2019) 008, [arXiv:1809.04517 \[hep-ph\]](#).
- [27] N. Byers and C. N. Yang, “Physical Regions in Invariant Variables for n Particles and the Phase-Space Volume Element,” *Rev. Mod. Phys.* **36** no. 2, (1964) 595–609.
- [28] W. S. Cho, J. S. Gainer, D. Kim, S. H. Lim, K. T. Matchev, F. Moortgat, L. Pape, and M. Park, “OPTIMASS: A Package for the Minimization of Kinematic Mass Functions with Constraints,” *JHEP* **01** (2016) 026, [arXiv:1508.00589 \[hep-ph\]](#).
- [29] C. B. Park, “YAM2: Yet another library for the  $M_2$  variables using sequential quadratic programming,” *Comput. Phys. Commun.* **264** (2021) 107967, [arXiv:2007.15537 \[hep-ph\]](#).
- [30] S. H. Lim, “Identifying the production process of new physics at colliders; symmetric or asymmetric?,” *JHEP* **06** (2016) 105, [arXiv:1603.01981 \[hep-ph\]](#).
- [31] C. Lester and A. Barr, “ $m_{T\text{Gen}}$ : Mass scale measurements in pair-production at colliders,” *JHEP* **12** (2007) 102, [arXiv:0708.1028 \[hep-ph\]](#).
- [32] W. S. Cho, K. Choi, Y. G. Kim, and C. B. Park, “Measuring superparticle masses at hadron collider using the transverse mass kink,” *JHEP* **02** (2008) 035, [arXiv:0711.4526 \[hep-ph\]](#).
- [33] W. S. Cho, K. Choi, Y. G. Kim, and C. B. Park, “Mass and Spin Measurement with  $M_{T2}$  and MAOS Momentum,” *Nucl. Phys. B Proc. Suppl.* **200-202** (2010) 103–112, [arXiv:0909.4853 \[hep-ph\]](#).
- [34] C. G. Lester, “The transverse mass,  $M_{T2}$ , in special cases,” *JHEP* **05** (2011) 076, [arXiv:1103.5682 \[hep-ph\]](#).
- [35] C. H. Lally and C. G. Lester, “Properties of  $M_{T2}$  in the massless limit,” [arXiv:1211.1542 \[hep-ph\]](#).



- [36] W. S. Cho, K. Choi, Y. G. Kim, and C. B. Park, “Gluino Stransverse Mass,” *Phys. Rev. Lett.* **100** (2008) 171801, [arXiv:0709.0288 \[hep-ph\]](#).
- [37] A. J. Barr, B. Gripaios, and C. G. Lester, “Weighing Wimps with Kinks at Colliders: Invisible Particle Mass Measurements from Endpoints,” *JHEP* **02** (2008) 014, [arXiv:0711.4008 \[hep-ph\]](#).
- [38] M. Burns, K. Kong, K. T. Matchev, and M. Park, “Using Subsystem  $M_{T2}$  for Complete Mass Determinations in Decay Chains with Missing Energy at Hadron Colliders,” *JHEP* **03** (2009) 143, [arXiv:0810.5576 \[hep-ph\]](#).
- [39] P. Konar, K. Kong, K. T. Matchev, and M. Park, “Dark Matter Particle Spectroscopy at the LHC: Generalizing  $M_{T2}$  to Asymmetric Event Topologies,” *JHEP* **04** (2010) 086, [arXiv:0911.4126 \[hep-ph\]](#).
- [40] R. Mahbubani, K. T. Matchev, and M. Park, “Re-interpreting the Oxbridge stransverse mass variable  $M_{T2}$  in general cases,” *JHEP* **03** (2013) 134, [arXiv:1212.1720 \[hep-ph\]](#).
- [41] W. S. Cho, K. Choi, and C. B. Park, “The  $M_{T2}$  solution to the invisible particle momenta in balanced configuration,” Unpublished.
- [42] K. Choi, S. Choi, J. S. Lee, and C. B. Park, “Reconstructing the Higgs boson in dileptonic W decays at hadron collider,” *Phys. Rev. D* **80** (2009) 073010, [arXiv:0908.0079 \[hep-ph\]](#).
- [43] K. Choi, J. S. Lee, and C. B. Park, “Measuring the Higgs boson mass with transverse mass variables,” *Phys. Rev. D* **82** (2010) 113017, [arXiv:1008.2690 \[hep-ph\]](#).
- [44] B. Buchberger, “A theoretical basis for the reduction of polynomials to canonical forms,” *ACM SIGSAM Bulletin* **10** (1976) 19–29.
- [45] CMS Collaboration, G. L. Bayatian *et al.*, “CMS technical design report, volume II: Physics performance,” *J. Phys. G* **34** no. 6, (2007) 995–1579.
- [46] M. M. Nojiri, Y. Shimizu, S. Okada, and K. Kawagoe, “Inclusive transverse mass analysis for squark and gluino mass determination,” *JHEP* **06** (2008) 035, [arXiv:0802.2412 \[hep-ph\]](#).
- [47] A. Rajaraman and F. Yu, “A New Method for Resolving Combinatorial Ambiguities at Hadron Colliders,” *Phys. Lett. B* **700** (2011) 126–132, [arXiv:1009.2751 \[hep-ph\]](#).
- [48] P. Baringer, K. Kong, M. McCaskey, and D. Noonan, “Revisiting Combinatorial Ambiguities at Hadron Colliders with  $M_{T2}$ ,” *JHEP* **10** (2011) 101, [arXiv:1109.1563 \[hep-ph\]](#).

- [49] K. Choi, D. Guadagnoli, and C. B. Park, “Reducing combinatorial uncertainties: A new technique based on  $M_{T2}$  variables,” *JHEP* **11** (2011) 117, [arXiv:1109.2201 \[hep-ph\]](#).
- [50] D. Debnath, D. Kim, J. H. Kim, K. Kong, and K. T. Matchev, “Resolving Combinatorial Ambiguities in Dilepton  $t\bar{t}$  Event Topologies with Constrained  $M_2$  Variables,” *Phys. Rev. D* **96** no. 7, (2017) 076005, [arXiv:1706.04995 \[hep-ph\]](#).
- [51] C. B. Park, “Reconstructing the heavy resonance at hadron colliders,” *Phys. Rev. D* **84** (2011) 096001, [arXiv:1106.6087 \[hep-ph\]](#).
- [52] C. G. Lester and B. Nachman, “Bisection-based asymmetric  $M_{T2}$  computation: a higher precision calculator than existing symmetric methods,” *JHEP* **03** (2015) 100, [arXiv:1411.4312 \[hep-ph\]](#).
- [53] **ATLAS** Collaboration, G. Aad *et al.*, “Search for electroweak production of charginos and sleptons decaying into final states with two leptons and missing transverse momentum in  $\sqrt{s} = 13$  TeV  $pp$  collisions using the ATLAS detector,” *Eur. Phys. J. C* **80** no. 2, (2020) 123, [arXiv:1908.08215 \[hep-ex\]](#).
- [54] **CMS** Collaboration, A. M. Sirunyan *et al.*, “Search for supersymmetry in final states with two oppositely charged same-flavor leptons and missing transverse momentum in proton-proton collisions at  $\sqrt{s} = 13$  TeV,” *JHEP* **04** (2021) 123, [arXiv:2012.08600 \[hep-ex\]](#).
- [55] T. Sjöstrand, S. Ask, J. R. Christiansen, R. Corke, N. Desai, P. Ilten, S. Mrenna, S. Prestel, C. O. Rasmussen, and P. Z. Skands, “An introduction to PYTHIA 8.2,” *Comput. Phys. Commun.* **191** (2015) 159–177, [arXiv:1410.3012 \[hep-ph\]](#).